

Effect of Toroidal Current on Rotational Transform Profile by MHD Activity Measurement in Heliotron J

Gen MOTOJIMA, Satoshi YAMAMOTO¹⁾, Hiroyuki OKADA²⁾, Satoru SAKAKIBARA³⁾, Kiyomasa WATANABE³⁾, Kazunobu NAGASAKI²⁾, Yasuhiro SUZUKI³⁾, Tohru MIZUUCHI²⁾, Shinji KOBAYASHI²⁾, Boyd D. BLACKWELL⁴⁾, Yuji NAKAMURA, Katsumi KONDO, Kiyoshi HANATANI²⁾, Hajime ARIMOTO, Shinya WATANABE and Fumimichi SANNO²⁾

Graduate School of Energy Science, Kyoto University, Uji 611-0011, Japan

¹⁾*Kyoto University Pioneering Research Unit for Next Generation, Uji 611-0011, Japan*

²⁾*Institute of Advanced Energy, Kyoto University, Uji 611-0011, Japan*

³⁾*National Institute for Fusion Science, Toki 509-5292, Japan*

⁴⁾*Plasma Research Laboratory, Research School of Physical Sciences and Engineering, The Australian National University, Canberra ACT 0200, Australia*

(Received 16 November 2007 / Accepted 4 February 2008)

The effect of toroidal current on the rotational transform was investigated in Heliotron J by measuring magnetohydrodynamic (MHD) activities at two configurations with a rotational transform ($\iota/2\pi$) close to 0.5. The resonant $m/n = 2/1$ mode was observed in an ECH + co-NBI plasma in the configuration with $\iota/2\pi = 0.48$ at $\rho = 0.7$. Here, m and n are the poloidal and toroidal mode numbers, respectively. ρ is the normalized minor radius. The rotational transform is increased presumably due to the toroidal current. The location of the $\iota/2\pi = 0.50$ rational surface was determined to be $\rho = 0.8-0.9$ by soft X-ray (SX) fluctuations related to the MHD mode. An equilibrium calculation considering the toroidal current showed that the increase in the rotational transform due to the toroidal current was consistent with experimental results. The resonant mode structure was also investigated in an ECH + counter-NBI plasma at the $\iota/2\pi = 0.50$ configuration. The location of the $\iota/2\pi = 0.50$ rational surface, as determined by SX signals, did not change significantly compared with that obtained under a vacuum configuration. There is no significant difference between the rotational transform profile that considers toroidal currents by equilibrium calculation and that of the vacuum configuration. These results suggest that the change in the rotational transform profile caused by the toroidal current was small, owing to the balance between the bootstrap current and counter-flowing NB driven current.

© 2008 The Japan Society of Plasma Science and Nuclear Fusion Research

Keywords: bootstrap current, NB driven current, MHD instability, magnetic fluctuation, Heliotron J

DOI: 10.1585/pfr.3.S1067

1. Introduction

Suppression of magnetohydrodynamic (MHD) instability is important for achieving high-performance plasmas. In helical plasmas, stabilization of pressure-driven modes, such as ideal and/or resistive interchange modes, is a critical issue for a high- β plasma. Heliotron J is a low magnetic shear helical-axis heliotron device with a magnetic well, which is expected to help avoid or minimize MHD instability [1]. However, MHD instabilities have been experimentally observed in plasmas heated by electron cyclotron heating (ECH) and neutral beam injection (NBI) [2]. The $m/n = 2/1$ MHD instability, exhibiting intense magnetic fluctuations and a frequency of $f < 10$ kHz, has been observed in plasmas with a rotational transform ($\iota/2\pi$) close to 0.5, where m and n are the poloidal and toroidal mode numbers, respectively. The equilibrium configuration is changed by the toroidal current and plasma

pressure, and a low-order resonant rational surface can appear in the plasma. Toroidal currents, such as the bootstrap current, electron cyclotron (EC) driven current, and neutral beam (NB) driven current, have been examined in Heliotron J [3, 4]. Such currents can modify the MHD equilibrium and stability due to the change in the rotational transform profile. The effects of the toroidal current on MHD modes have been investigated in CHS [5] and W7-AS [6]. In Heliotron J, the approach to the transition to an improved confinement mode has been investigated [7]. The transition in NBI-only plasma has been recently investigated. The experiments show that the transition occurs at a certain value of the toroidal current [8]. The modification of the rotational transform by the toroidal current may induce a spontaneous transition. The objective of the present paper is to study the effect of toroidal current on the rotational transform by measuring MHD activities in Heliotron J.

author's e-mail: gen@center.iae.kyoto-u.ac.jp

The organization of the rest of the paper is as follows. The experimental setup is described in Section 2. In Section 3, the experimental results for the resonant $m/n = 2/1$ mode in ECH + NBI plasmas are discussed. In addition, separation of the bootstrap current and the NB driven current is also presented. In Section 4, we discuss the effect of toroidal current on the rotational transform by equilibrium calculations. We present the conclusions in Section 5.

2. Experimental Setup

Heliotron J is a medium-sized plasma experimental device. Figure 1 shows the top-view of the Heliotron J device. The device parameters are as follows: plasma major radius $R = 1.2$ m, averaged minor radius $a = 0.1$ - 0.2 m, ro-

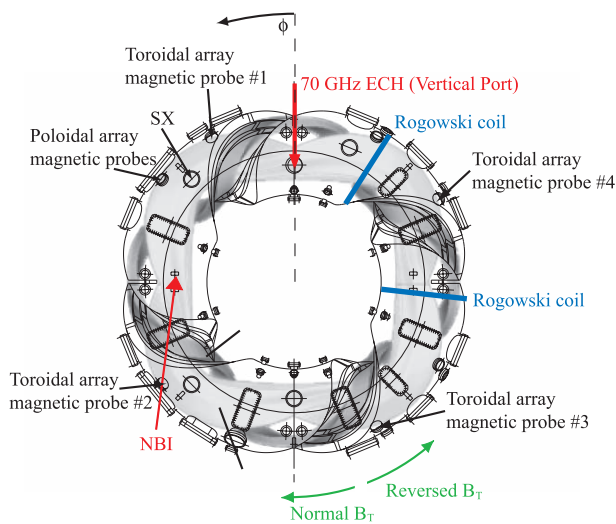


Fig. 1 Top view of Heliotron J device. The positions of the heating systems and some diagnostics are shown. Equivalent current is counterclockwise direction by vacuum poloidal magnetic field.

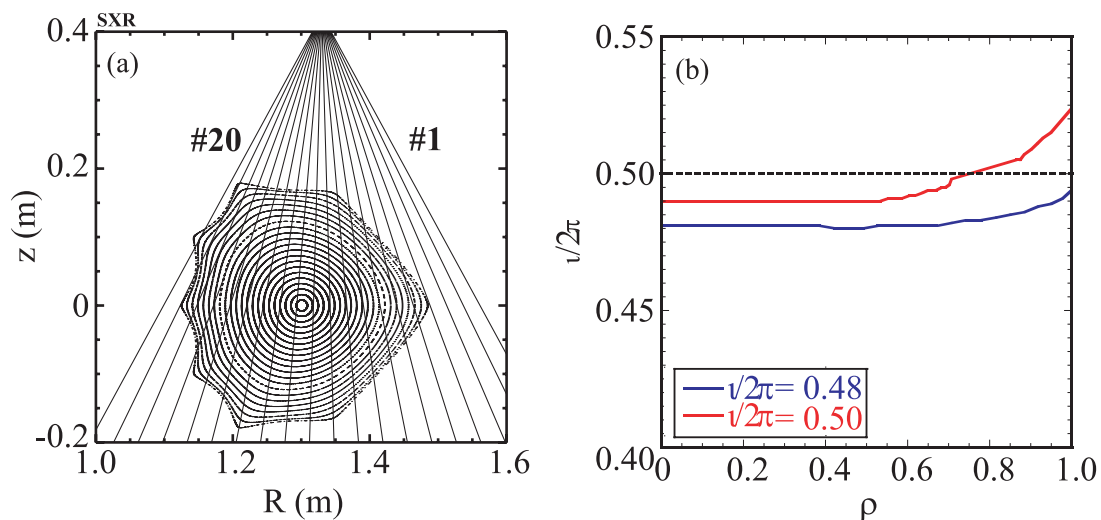


Fig. 2 (a) Magnetic flux surface and 20 lines of sight in the SX array. (b) Radial profiles of the rotational transform under vacuum conditions.

tational transform $\iota/2\pi = 0.3$ - 0.8 , and the maximum magnetic field strength on the magnetic axis $B_0 = 1.5$ T. The coil system is composed of a helical coil with $L = 1$ and $M = 4$, two types of toroidal coils, and three pairs of vertical coils. Here, L is the pole number of the helical coil, and M is the pitch number of the field along the toroidal direction. A wide variety of magnetic configurations can be produced on the Heliotron J by controlling each current flowing in these coils. In this study, two configurations with the rotational transform close to 0.5 were selected, namely, $\iota/2\pi = 0.48$ and 0.50 at $\rho = 0.7$ under vacuum conditions, while the major Fourier components in the Boozer coordinates of the confinement field were kept almost constant. Here, ρ is the normalized minor radius. In Fig. 2(a), the poloidal cross section of toroidal angle $\phi = 45^\circ$ for the $\iota/2\pi = 0.48$ configuration is shown, where the soft X-ray (SX) detector is located. Figure 2(b) shows the rotational transform profiles in the vacuum configuration. The total toroidal current is measured using Rogowski coils wound on the inner wall of the poloidal cross sections at two different toroidal angles. We define the positive toroidal current as co-direction and the negative current as counter-direction. Here, “co-” means the toroidal current increases the vacuum rotational transform, and “counter-” means the toroidal current decreases the vacuum rotational transform. To produce the plasma, NB was injected into the ECH plasma (ECH + NBI plasma). Here, NB was injected in the counter-direction in the case of the normal magnetic field. When the magnetic field is reversed, NB was injected in the co-direction. For determining the geometric structure of magnetic fluctuations accurately, four Mirnov coils are installed in the toroidal direction and 14 mirnov coils are set poloidally on one poloidal cross-section. The magnetic probes have a frequency response of up to 500 kHz. A SX diode array has 20 vertical viewing chords. Figure 2(a) shows the lines of sight of the SX array.

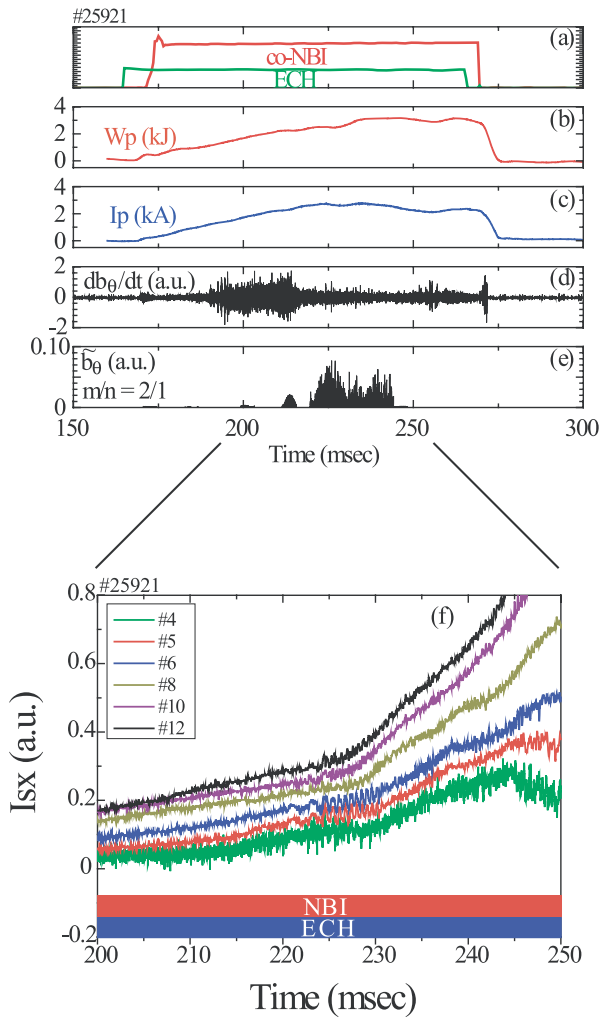


Fig. 3 Time evolution of an ECH + co-NBI plasma. The (a) NBI and ECH, (b) stored energy, (c) plasma current, (d) Mirnov signal, (e) Magnetic fluctuation of $m/n = 2/1$ mode, and (f) SX signal.

3. Experimental Results

3.1 ECH + co-NBI plasma

Figure 3 shows a discharge with ECH + co-NBI for the $\iota/2\pi = 0.48$ configuration. An ECH power of 208 kW is injected from 165 to 265 ms. An NB port-through power of 573 kW is injected from 175 to 265 ms. The net toroidal current is increased up to 2.5 kA in the co-direction. The magnitude fluctuation of $m/n = 2/1$ mode with a frequency of 3 kHz is observed from 225 to 245 ms. The $m/n = 2/1$ mode rotates in the electron diamagnetic direction. The fluctuation of the SX signal also appears simultaneously, as shown in Fig. 3(f). Figure 4(a) shows the relative amplitude of the fluctuations δI_{SX} , observed in the SX signal. Peaks are observed at #5 ($\rho = 0.90$), #15 ($\rho = 0.45$), and #18 ($\rho = 0.80$). Figure 4(b) shows the phase difference between the SX channels for the mode. The derived phase relation indicates the “even” or “odd” character of the m number: the phase difference between the SX channels is $\sim 2\pi$ ($\sim \pi$) for an even (odd) m number. The phases

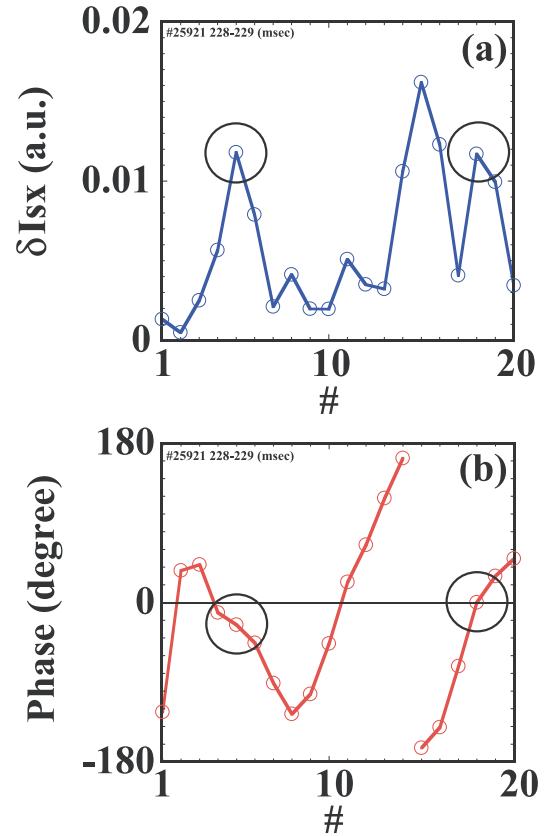


Fig. 4 Radial profile of (a) SX fluctuation amplitude and (b) phase difference between SX channels in ECH + co-NBI plasma.

#5 and #18, are almost the same, and they are consistent with $m = 2$, which is determined using the magnetic probe arrays. Therefore, they correspond to the location of the resonant surface of the $m/n = 2/1$ mode. The intensity of #15 is high. The phase difference between #15 and #5 (#18) is $\sim \pi$. However, the details remain unclear. In the vacuum magnetic surface of the $\iota/2\pi = 0.48$ configuration, there is no rational surface of the $m/n = 2/1$; however, the rotational transform is affected by the plasma pressure and co-flowing toroidal current, resulting in crossing of the rational surface of the $m/n = 2/1$ mode. The movement of the peak position of δI_{SX} is not observed. The $m/n = 2/1$ mode is not observed after 245 ms. The rational surface of $m/n = 2/1$ may disappear due to the decrease in rotational transform induced by the slight reduction of toroidal current.

3.2 ECH + counter-NBI plasma

Figure 5 shows a discharge in ECH + counter-NBI with the $\iota/2\pi = 0.50$ configuration. An ECH pulse with a power of 312 kW is injected from 165 to 290 ms. The NB with a port-through power of 561 kW is injected from 170 to 290 ms. The net toroidal current is increased up to 1 kA in the co-direction. The total toroidal current during counter-NBI injection is smaller than that during co-NBI

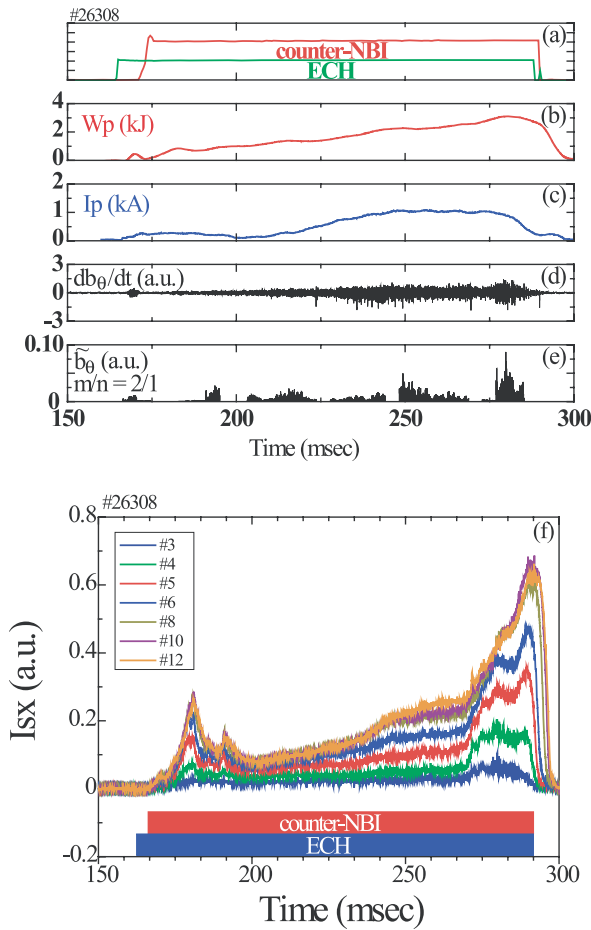


Fig. 5 Time evolution of an ECH + counter-NBI plasma. The (a) NBI and ECH, (b) stored energy, (c) plasma current, (d) Mirnov signal, (e) Magnetic fluctuation of $m/n = 2/1$ mode, and (f) SX signal.

injection, since the NB driven current flows in the counter-direction against the bootstrap current. The $m/n = 2/1$ mode with a frequency of 5 kHz is observed from 165 to 280 ms. The mode rotates in the electron diamagnetic direction. The fluctuation in the SX signal also appears simultaneously, as shown Fig. 5(f). Figure 6 shows the relative amplitude of the fluctuations observed in the SX signal at 287-288 ms, when the $m/n = 2/1$ mode is the strongest. The peak is observed at 3 and 19 ch. The phases of 3 and 19 ch are almost the same, which is consistent with $m = 2$, which is identified by magnetic probes. No shift of the peak has been observed, similar to the case of ECH + co-NBI plasma. The positions are almost identical to the rational surface of 0.5 in the vacuum configuration. This suggests that the position of the rational surface does not move, even though the finite net current exists.

3.3 Separation of the bootstrap current and NB driven current

In ECH + NBI plasmas, the toroidal current is composed of the bootstrap current and the NB driven current. These currents can be evaluated by comparing the exper-

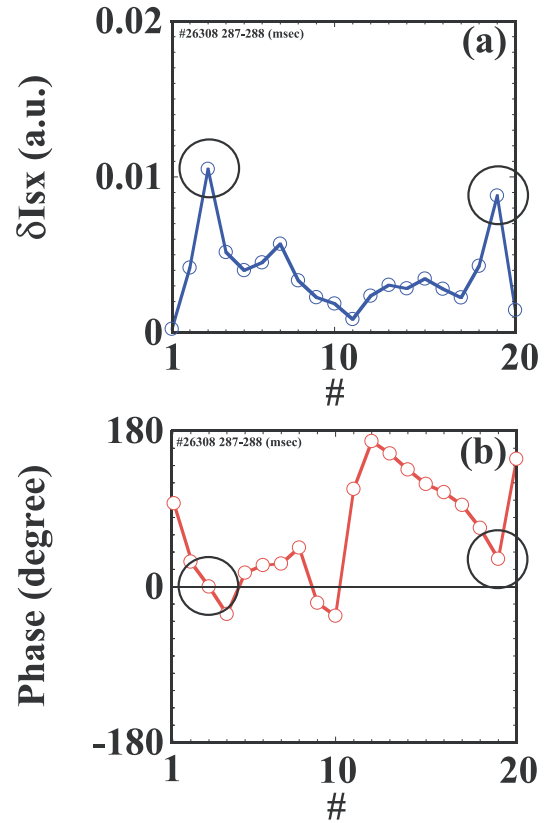


Fig. 6 Radial profile of (a) SX fluctuation amplitude and (b) phase difference between SX channels in ECH + counter-NBI plasma.

imental results obtained for the normal and the reversed magnetic fields, since the direction of the bootstrap current flows in co-direction for both cases, whereas the direction of the NB driven current is associated with the injected direction. Under the experimental conditions used in this study, the effect of the EC driven current is weak. The toroidal current for normal magnetic field I_p^{norm} is given by

$$I_p^{\text{norm}} = I_{BS} + I_{NB}^{\text{counter}}, \quad (1)$$

where I_{BS} is the bootstrap current, and I_{NB}^{counter} is the counter-flowing NB driven current. The toroidal current for reversed magnetic field I_p^{rev} is given by

$$I_p^{\text{rev}} = I_{BS} + I_{NB}^{\text{co}}, \quad (2)$$

where I_{NB}^{co} is the co-flowing NB driven current.

If we assume that $I_{NB}^{\text{counter}} = -I_{NB}^{\text{co}}$, we obtain the bootstrap current and NB driven current using Eqs. (1) and (2).

$$I_{BS} = \frac{I_p^{\text{norm}} + I_p^{\text{rev}}}{2}, \quad (3)$$

$$I_{NB}^{\text{counter}} = \frac{I_p^{\text{norm}} - I_p^{\text{rev}}}{2}. \quad (4)$$

We confirmed that the stored energies of the normal and reversed magnetic fields were almost identical. However, we should note that the absorption rate of NB is affected by the direction of the magnetic field, due to the change

in the loss rate of high energy ions. Figure 7 shows approximate evaluations of the bootstrap and NB driven currents. The bootstrap current is 1.5 ± 0.2 kA for $\iota/2\pi = 0.48$ and 1.8 ± 0.3 kA for $\iota/2\pi = 0.50$, whereas the co-flowing (counter-flowing) NB driven current is 1.0 (-1.0) ± 0.2 kA for $\iota/2\pi = 0.48$ and 0.8 (-0.8) ± 0.3 kA for $\iota/2\pi = 0.50$.

4. Discussions

To determine the effect of the toroidal current on the equilibrium, fixed boundary VMEC calculations considering the toroidal current were carried out [9]. The electron density is given by $n_e = 2 \times 10^{19}(1 - s^3) \text{ m}^{-3}$, and the electron and ion temperatures are given by $T_e = 0.45 \times (1 - s)^2 \text{ keV}$ and $T_i = 0.15 \times (1 - s)^2 \text{ keV}$, respectively. Here, s denotes the normalized toroidal flux, and the relationship $s = \rho^2$ holds. We assume these profiles, since the pressure profile has not been obtained yet. Figure 8(a) shows the bootstrap current and NB driven current profiles.

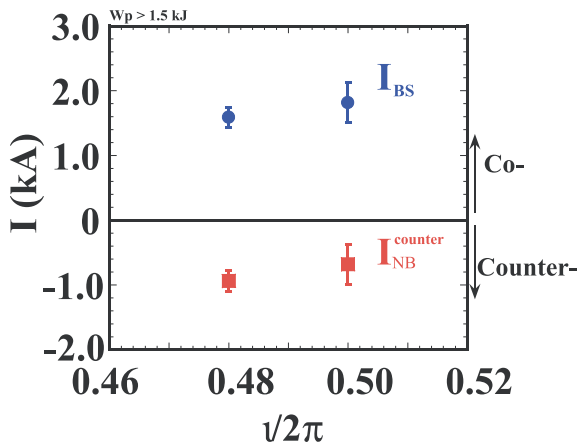


Fig. 7 Estimated bootstrap current and NB driven current.

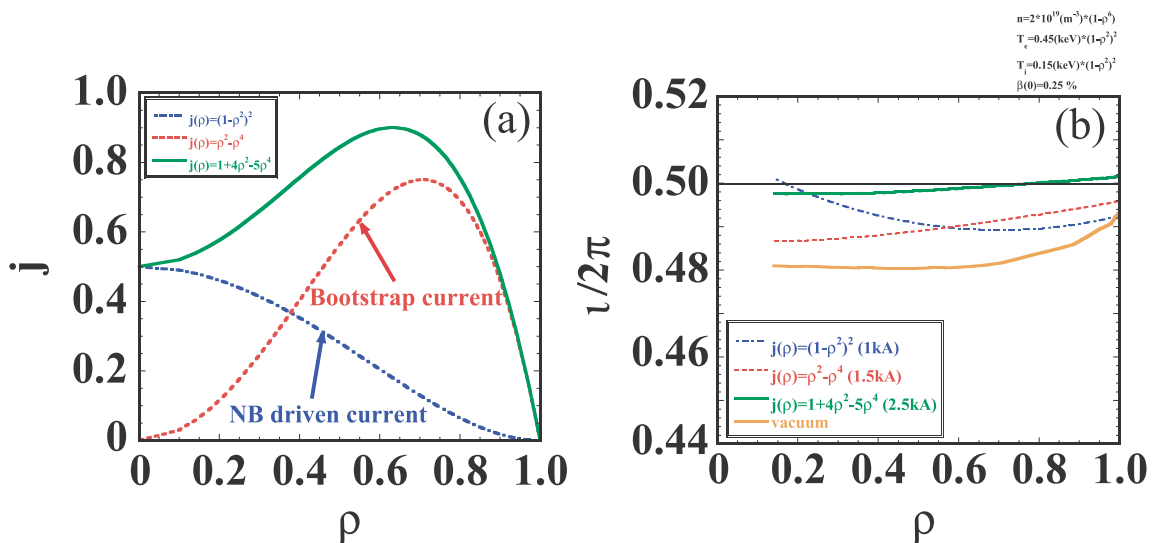


Fig. 8 (a) Toroidal current profile and (b) radial profile of rotational transform determined by VMEC calculation with the effect of toroidal current and plasma pressure in ECH + co-NBI plasma.

We assumed that the bootstrap current density is given by $j = j_0(s - s^2)$ since the bootstrap current may flow at off-axis, where the plasma pressure gradient is large. The NB driven current is given by $j = j_0(1 - s)^2$, since the deposition of NB may be on-axis. Each value of the bootstrap and NB driven current was estimated using Eqs. (3) and (4). Figure 8(b) shows the radial profile of the rotational transform calculated using the VMEC code with toroidal current in ECH + co-NBI plasma. When a bootstrap current of 1.5 kA and an NB driven current of 1 kA flow in the co-direction, the rotational transform profile has the rational surface of the $m/n = 2/1$ mode around $\rho = 0.8$. The calculated location of the rational surface of the $m/n = 2/1$ is consistent with that obtained from the SX signals.

The VMEC calculations were also performed in ECH + counter-NBI plasma. The profiles of toroidal currents and plasma pressure were similar to those of ECH + co-NBI plasma. Figure 9 shows the calculated rotational transform profile with toroidal current. There is no significant difference between the rotational transform profile that considers the toroidal currents and that of the vacuum configuration, when compared with the ECH + co-NBI plasma. These results suggest that the change in the rotational transform profile induced by the toroidal current is small, owing to the balance between the bootstrap current and counter-flowing NB driven current.

5. Conclusion

The effect of toroidal current on the rotational transform was studied in Heliotron J by measuring MHD activities. In an ECH + co-NBI plasma with $\iota/2\pi = 0.48$ configuration, the $m/n = 2/1$ mode with frequency of $f = 3$ kHz was observed when the co-flowing toroidal current was increased to 2.5 kA. The rotational transform presumably increased due to the toroidal current, resulting in

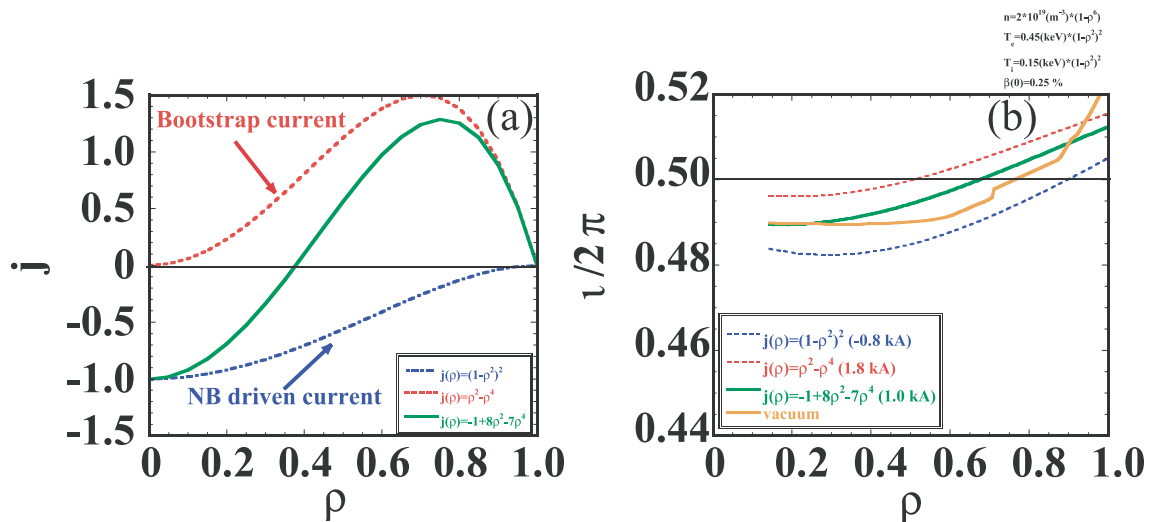


Fig. 9 (a) Toroidal current profile and (b) radial profile of rotational transform deduced from VMEC calculation with the effect of toroidal current and plasma pressure in ECH + counter-NBI plasma.

crossing of the rational surface of $\nu/2\pi = 1/2$. Measurement of the mode structure using a 20-channel SX detector array showed that the rational surface was located around $\rho = 0.8-0.9$. The increase of the rotational transform by the toroidal current is consistent with the equilibrium calculations. The $m/n = 2/1$ mode was also observed in the ECH + counter-NBI plasma with $\nu/2\pi = 0.50$ configuration. By an SX measurement, the position of the rational surface was determined to be unchanged from that of the vacuum configuration. Equilibrium calculations also showed that there is no significant change in the rotational transform profile due to the toroidal current. These results suggest that the change in the rotational transform profile induced by the assumed current profiles is small in the ECH + counter-NBI plasma, because the counter-flowing NB driven current density decreases the rotational

transform. The assumed bootstrap current and NB driven current profiles are considered to be valid. However, we will discuss the effect of some current density profiles on the rotational transform in the future.

- [1] T. Obiki *et al.*, Nucl. Fusion **41**, 833 (2001).
- [2] S. Yamamoto *et al.*, Fusion Sci. Technol. **51**, 92 (2007).
- [3] G. Motojima *et al.*, Nucl. Fusion **47**, 1045 (2007).
- [4] G. Motojima *et al.*, Fusion Sci. Technol. **51**, 122 (2007).
- [5] S. Sakakibara *et al.*, Jpn. J. Appl. Phys. **34**, L252 (1995).
- [6] E. Sallander *et al.*, Nucl. Fusion **40**, 1499 (2000).
- [7] F. Sano *et al.*, Nucl. Fusion **45**, 1557 (2005).
- [8] S. Kobayashi *et al.*, Proc. 34th EPS Conf. on plasma Phys. Warsaw, ECA **31F**, P-4. 162 (2007); also available at http://epsppd.epfl.ch/Warsaw/pdf/P4_162.pdf
- [9] S.P. Hirshman and O. Betancourt, J. Comput. Phys. **96**, 99 (1991).